Beta asymmetry of the first forbidden $\frac{1}{2}^+ \rightarrow \frac{1}{2}^-$ transition in ^{19}Ne and its relationship to the parity nonconserving nucleon-nucleon interaction

E. R. J. Saettler,* F. P. Calaprice, A. L. Hallin,† and M. M. Lowry
Joseph Henry Laboratories, Princeton University, Princeton, New Jersey 08544
(Received 9 July 1993)

We report a measurement of the β asymmetry of the first-forbidden transition from the $\frac{1}{2}^+$ ground state of ^{19}Ne to the $\frac{1}{2}^-$ level at 110 keV in ^{19}F. Using atomic beam methods to prepare a 100% polarized source of ^{19}Ne, we identify the $\frac{1}{2}^+ \rightarrow \frac{1}{2}^-$ decays by the detection of the subsequent 110 keV gamma emitted in coincidence with a beta. The average β asymmetry of the first-forbidden transition is measured to be $\langle A \rangle = 17 \pm 12\,\%$. We simultaneously make an improved measurement of the branching ratio of the same transition and find $\Gamma = (1.13 \pm 0.09) \times 10^{-4}$ in good agreement with previous results. Our measurement is used to obtain an improved calibration of the isovector parity-mixing matrix element between the $\frac{1}{2}^+$ ground state of ^{19}F and the $\frac{1}{2}^-$ level at 110 keV.

PACS number(s): 23.40.Hc, 27.20.+n

I. INTRODUCTION

Below about 300 MeV the effective weak interaction between nucleons can be described by the exchange of a single meson (π^0, ρ, or ω) between two nucleons with one strong interaction vertex and one weak vertex. Desplanques *et al.* [1] have calculated the weak parity-violating nucleon-meson couplings from the standard model. Coupling constants for this parity nonconserving nucleon-nucleon (PNC-NN) interaction are denoted $h_\rho^{0,1,2}$, $h_\omega^{0,1}$, and f_π; the superscript indicating the isospin change, the subscript the meson exchanged. The pion-exchange coupling, f_π, is purely isovector. The experimental determination of these couplings is an important test of our understanding of the weak interaction between quarks.

Important constraints on parity-violating couplings have come from measurements of parity-mixed doublets in ^{18}F [2,3], ^{19}F [4,5], and ^{21}Ne [6]. The single positive result of parity mixing in a light nucleus is the parity mixing between the $(J^\pi; I = 1/2^+; 1/2)$ ground state of ^{19}F and the $(1/2^-; 1/2)$ first excited state at 110 keV. This is derived from the measured angular asymmetry of the $E1$ gamma transition between these states. Parity mixing in ^{18}F is purely isovector, and measurements on this nucleus set a limit on the dominant isovector coupling, f_π, which is an order of magnitude smaller than the theoretical "best value."

In order to relate parity-violating observables in light nuclei to the weak meson-nucleon couplings it is necessary to know the nuclear matrix elements of the operators in the PNC-NN potential. Nuclear shell-model calculations have not yielded consistent evaluations of these matrix elements. Fortunately, it is possible in the $A = 18$ and 19 systems to use analog beta decays to "calibrate" the nuclear matrix elements so that nuclear structure uncertainties may be removed from the effective weak-coupling constants. Our measurement of the beta asymmetry of the analog first-forbidden beta decay, together with a more precise determination of the branching ratio, provide an improved calibration of the nuclear matrix elements in the $A = 19$ system.

The possibility of such a model-independent calibration was originally pointed out by Bennett, Lowry, and Krien [7]. The isovector pion-exchange term of the PNC-NN interaction, $V_\pi^{\rm PNC}$, is identical, apart from coupling constants and rotation in isospin space, to the two-body pion-exchange contribution to the axial-charge matrix element $\langle \gamma_5 \rangle$ of first-forbidden β decay [8–10]:

$$V_\pi^{\rm PNC} = \frac{i f_\pi g_{\pi NN}}{2\sqrt{2}} (\boldsymbol{\tau}_1 \times \boldsymbol{\tau}_2)_3 (\boldsymbol{\sigma}_1 + \boldsymbol{\sigma}_2) \cdot \left[\frac{\mathbf{p}_1 - \mathbf{p}_2}{2M}, \phi_\pi(r) \right] , \tag{1}$$

$$\lambda \langle \gamma_5 \rangle = \lambda \langle \gamma_5; \text{one-body} \rangle + \frac{i\, g_{\pi NN}^2}{2\sqrt{2}\lambda M} (\boldsymbol{\tau}_1 \times \boldsymbol{\tau}_2)_\pm (\boldsymbol{\sigma}_1 + \boldsymbol{\sigma}_2) \cdot \left[\frac{\mathbf{p}_1 - \mathbf{p}_2}{2M}, \phi_\pi(r) \right] , \tag{2}$$

where

$$\phi_\pi(r) = \exp(-m_\pi r)/4\pi r \, . \tag{3}$$

$\boldsymbol{\sigma}_i$ and $\boldsymbol{\tau}_i$ are Pauli spin and isospin matrices, respectively, for the ith nucleon; $g_{\pi NN} = 13.45$ is the strong coupling; $M = 1840$ is the nucleon mass in units of $m_e c^2$;

*Present address: TRIUMF, 4004 Wesbrook Mall, Vancouver, British Columbia, Canada V6T 2A3.
†Present address: Queens University Physics Department, Kingston, Ontario, Canada K7L 3N6.

and $\lambda = 1.2605$ [11] is the ratio of hadronic axial-vector to vector weak-coupling constants. Haxton [4] has shown for the transitions of interest that, although the magnitude of the $\langle\gamma_5\rangle$ matrix element varies greatly in different calculations, the ratio of one- to two-body contributions is relatively model *independent*. Such analogue first-forbidden beta transitions exist for ^{18}F and ^{19}F but not for ^{21}Ne. Adelberger *et al.* [12,13] measured the branching ratio of these first-forbidden β decays. Their measured branching ratio for analogue first-forbidden β^+ transition in ^{19}F (see Fig. 1) is $\Gamma = (1.2 \pm 0.2) \times 10^{-4}$.

In the case of the first parity-forbidden β decay of ^{19}Ne with $J_i = J_f = 1/2$ there are five nuclear matrix elements involved—two rank-0 and three rank-1 (see, for example, Konopinski [14]). The shape factor $C(W)$ is defined by the following equation for the rate:

$$\frac{d\lambda}{dW} = \frac{{G_\beta}^2}{2\pi^3}(W_0 - W)^2 pW F(Z,W) C(W) , \qquad (4)$$

where p, W are the electron momentum and energy; W_0 is the end-point energy; $F(Z,W)$ is the ratio of electron density at the nuclear radius for a charged over an uncharged nucleus. In the simplest approximation, the shape factor for this first-forbidden transition is energy independent, and is the sum of the squared total rank-0 and rank-1 matrix elements:

$$C = \zeta_0^2 + \zeta_1^2 , \qquad (5)$$

where, for β^+ decay,

$$\zeta_0 = -\lambda\langle\gamma_5\rangle - \lambda\langle i\boldsymbol{\sigma}\cdot\hat{\mathbf{r}}\rangle\left(\frac{\alpha Z}{3} - \frac{W_0 R}{3}\right) , \qquad (6)$$

$$\zeta_1 = -\langle\boldsymbol{\alpha}\rangle - \lambda\langle\boldsymbol{\sigma}\times\hat{\mathbf{r}}\rangle\left(\frac{\alpha Z}{3} + \frac{W_0 R}{3}\right) - \langle i\hat{\mathbf{r}}\rangle\left(\frac{\alpha Z}{3} - \frac{W_0 R}{3}\right) . \qquad (7)$$

The timelike axial-vector matrix element $\langle\gamma_5\rangle$ is the dominant term and is rank 0. In order to determine $\langle\gamma_5\rangle$ from the rate, one must evaluate the contributions of the other four matrix elements. Assuming a system with good isospin, two of the three rank-1 matrix elements

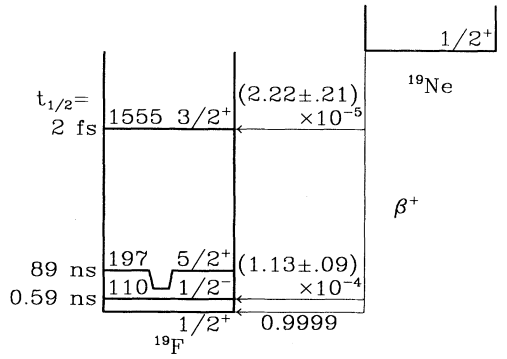

FIG. 1. ^{19}Ne beta-decay level diagram. (From Refs. [4,24].) The branching ratio for the decay to the $1/2^-$ state is from this work.

can be evaluated from analogue gamma transitions using the conserved vector current (CVC) hypothesis. Their contribution to the rate is small. However, the matrix elements $\langle\boldsymbol{\sigma}\times\hat{\mathbf{r}}\rangle$ and $\langle i\boldsymbol{\sigma}\cdot\hat{\mathbf{r}}\rangle$ may contribute significantly to the rate. In their analysis of the branching ratio Adelberger and Haxton have relied on shell-model calculations for these matrix elements. They find the total rank-1 contribution to the rate to be negligible [4]. The contribution of the remaining rank-0 term, $\langle i\boldsymbol{\sigma}\cdot\hat{\mathbf{r}}\rangle$, in the same analysis is about 10% of the total rate and adds constructively to $\langle\gamma_5\rangle$. While the relative contribution of $\langle i\boldsymbol{\sigma}\cdot\hat{\mathbf{r}}\rangle$ remains reasonably constant in a number of different models, none of these models predict the experimental rate within a factor of 3. Calculations by Millener and Warburton [15] using Woods-Saxon rather than harmonic oscillator wave functions differ significantly from those of Adelberger and Haxton. They find a significant ($\sim 20\%$) contribution to the rate from rank-1 terms and also a destructive rather than a constructive contribution from $\langle i\boldsymbol{\sigma}\cdot\hat{\mathbf{r}}\rangle$ of about 6% of $\langle\gamma_5\rangle$. These matrix elements predict a rate approximately 50% higher than the experimental value, without including the expected 40% enhancement in $\langle\gamma_5\rangle$ from pion-exchange currents.

The β-asymmetry A, the parity-violating angular correlation between the nuclear spin and the β direction, is defined by

$$d\lambda \propto [1 + A\,(v/c)\cos\theta]\, d\Omega , \qquad (8)$$

where θ is the angle between the nuclear spin and the β direction. In simplest approximation the β-asymmetry parameter is also energy independent and depends on a different combination of total rank-0 and rank-1 matrix elements. For a 100% polarized source and $J_i = J_f = 1/2$ the asymmetry is

$$A = \left[\frac{2}{3}\zeta_1^2 + \frac{2}{\sqrt{3}}\zeta_0\zeta_1\right] \Big/ C . \qquad (9)$$

With a measurement of the β asymmetry it is possible to separate the rank-0 from the rank-1 matrix elements. This removes the uncertainty in the contribution of rank-1 matrix elements to the rate. In addition, since two rank-1 terms are known through CVC, this effectively determines the third. It is not possible, with the present data, to separate the contribution of $\langle\gamma_5\rangle$ from the remaining rank-0 term; a shell-model calculation is required. The additional information provided by the measurement of the rank-1 matrix elements will help in testing and improving shell-model calculations of $\langle i\boldsymbol{\sigma}\cdot\hat{\mathbf{r}}\rangle$ in order to better determine $\langle\gamma_5\rangle$.

II. EXPERIMENT

A. Apparatus

^{19}Ne is produced and polarized using the Princeton rare gas atomic beam machine (Fig. 2). We will give only a brief description of this apparatus here as a more complete discussion has appeared previously [16,17]. ^{19}Ne

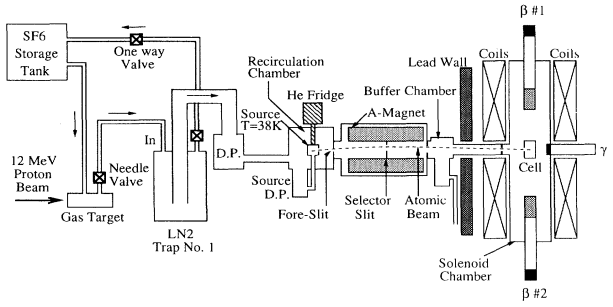

FIG. 2. Schematic of the experimental setup.

is produced via the $^{19}F(p,n)$ reaction by bombarding SF_6 gas with a 12 MeV proton beam from the Princeton cyclotron. The bombarded gas flows continuously to a liquid-nitrogen cold trap where the SF_6 is condensed. ^{19}Ne is pumped by a series of oil diffusion pumps to a cryogenic cell which is the atomic beam source. Nuclear polarization is achieved by deflecting the thermal-velocity atomic beam in a "Stern-Gerlach" magnet, the "A magnet." A beam with 100% nuclear polarization in either direction may be obtained by adjusting the position of a selector slit at the center of the A magnet. The atomic beam is captured in a holding cell at the center of a solenoid magnet. At this point 2.2 m from the source, the atomic beam is highly collimated and enters the cell through a long, narrow entrance channel. The cell is a cylinder 8.9 cm $\times$ 4.8 cm diameter made of Mylar (wall thickness = 10.3 mg/cm^2). The sitting time for ^{19}Ne in the cell was 6.5 ± 0.1 s. Nuclear depolarization during this time is negligible. With 45 μA of 12 MeV protons on target, the polarized ^{19}Ne decay rate in the cell is about 15 kHz.

At each end of the solenoid magnet is a plastic scintillator β detector of a special design described later in this section. Above the cell is a planar intrinsic germanium (HPGe) detector (1000 mm^2 $\times$ 10 mm). Energy and timing signals are derived from all three detectors. First-forbidden decays are identified by a coincidence between a beta and a 110 keV gamma from the decay of the final state. The β asymmetry is determined from the difference in rate between the forward and backward β detectors. After calibration of the germanium detector efficiency, the branching ratio of the first-forbidden transition may be obtained from the ratio of β-γ coincidences in the 110 keV peak to the total β's. Gamma energy resolution achieved in the experiment was 980 eV at 110 keV; timing resolution for β-γ coincidences was 32 ns (FWHM).

The solenoid magnet provides a uniform 4.1 kG field which allows the β detectors to be separated by about 1 m while still maintaining 4π acceptance for β's emitted from the cell. This is important for β backscatter reconstruction and for reducing the β-γ coincidence background due to annihilation radiation from the plastic scintillators which reaches the HPGe detector. Lead shielding is placed around the HPGe detector to block annihilation radiation from the detectors. The walls of the chamber are lined with lead to reduce the background due to Compton scattered 511's.

The β detectors were designed to minimize backscatter. They are in the shape of a 2 in. $\times$ 2 in. cross, 10 in. long, made of 1/4 in. Bicron BC400 scintillator. The cross is twisted 90° over its length so that all positron orbits will intersect with the vanes. Backscatters are kept to a minimum because β's tend to intersect the vanes at close to normal incidence. The orbit of a backscattered β is also likely to reintersect with the same detector somewhere along its length. Backscatters which escape one detector will orbit in the solenoid field to the other detector. Timing resolution of the plastic is sufficient to allow us to determine which detector was hit first. Energy resolution for the β detectors was 34% FWHM for 1 MeV positrons.

A small BGO crystal was positioned and collimated to detect annihilation radiation from the atomic beam source to be used as a monitor of the atomic beam intensity.

B. Electronics

About 97% of the total 15 kHz trigger rate in this experiment is due to β "singles" events—decays without a coincident gamma which do not backscatter. The remaining 3% "coincidence" events are primarily β-β coincidences generated by β backscatters, along with β-γ coincidences. In order to accommodate high data rates in this experiment and still perform essential reconstruction and sorting of the coincidence events, there were two alternative paths for the energy signals. One set of β- and γ-energy signals was converted by self-triggering LeCroy 3512 ADC's which were read by a LeCroy 3588 histogramming memory. Histograms were transferred to the main computer at the end of an acquisition cycle. This system was used for the "singles" events and had a dead time of about 5% at 15 kHz. A coincidence between the timing signals from two or more detectors (β or γ) triggered a second set of ADC's and TDC's which were read and sorted on line by the acquisition computer. The "singles" ADC's were vetoed by this trigger so that they recorded only the complimentary data set.

C. Data acquisition

Data are acquired in 50-min cycles; each cycle consisting of four phases or subcycles. In the first phase, polarized data are acquired for 20 min. In the second, a flag is inserted to block the atomic beam before it enters the cell and background data are taken for 5 min. The direction of polarization is then reversed by moving the selector slit in the A-magnet and another set of polarized data and background is acquired. The asymmetry calculation is performed as follows:

$$\Delta = A\langle v/c\rangle\langle\cos\theta\rangle \ , \tag{10}$$

where

$$\Delta = \frac{R^{1/2} - 1}{R^{1/2} + 1} \tag{11}$$

and

$$R = \frac{N(1,\uparrow)\,N(2,\downarrow)}{N(1,\downarrow)\,N(2,\uparrow)}. \tag{12}$$

N refers to a sum over the β spectrum after background subtraction; the numerical index indicates the detector number, the arrow nuclear polarization. The ratio R is insensitive to differences in efficiency between the two detectors and to differences in rate between the two polarization subcycles. The average $\langle \cos\theta \rangle$ is nominally 1/2; $\langle v/c \rangle$ must be determined from the energy calibration of the β detectors.

The β detectors are calibrated based on a fit to the ^{19}Ne β spectrum acquired during the run. Equally weighted spectra from both polarization subcycles were combined to produce an "unpolarized" β spectrum for each detector. In constructing the fitting function, we begin the β-spectrum statistical shape including a Fermi function and order-α radiative correction [18]. The effects of bremsstrahlung, annihilation-in-flight, and γ absorption are calculated by EGS4 Monte Carlo simulations [19,20]. The spectrum is then fit for energy gain, offset, and a Gaussian resolution width which increases as the square root of the energy. Satisfactory agreement with a calibration using a ^{207}Bi conversion-line source was obtained (see Fig. 3).

Before calculating the β asymmetry of the first-forbidden branch, data from all acquisition cycles are summed. Cuts are placed on the gamma timing and energy and background is subtracted based on sidebands (see Fig. 4). The asymmetry parameter of the first-forbidden transition is then calculated from Eqs. (10)–(12).

Because all β decays from the dominant superallowed

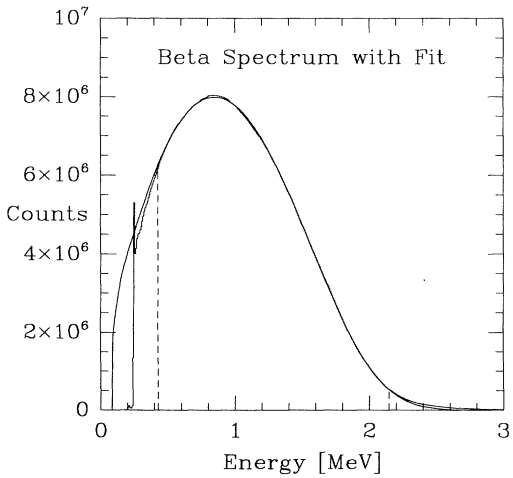

FIG. 3. Beta spectrum of the superallowed branch with energy-calibration fit. The effects of bremsstrahlung, annihilation-in-flight, and γ absorption were calculated by EGS4 Monte Carlo simulation [19,20]; the spectrum was then fit for energy gain, offset, and resolution width. Only the data between the dashed lines were used for the fit.

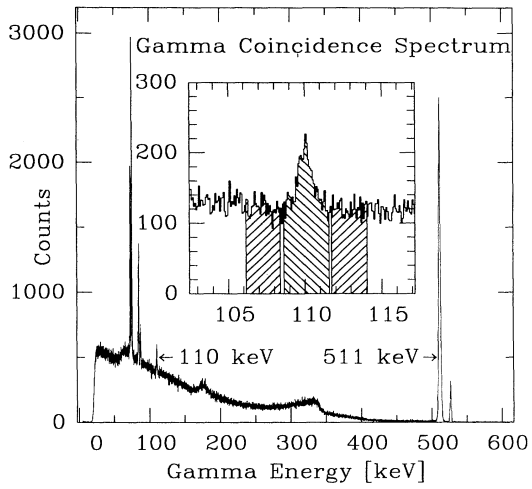

FIG. 4. Gamma energy spectrum of β-γ coincidences. The inset shows the cuts and sidebands for the branching-ratio analysis.

decay are also recorded during each polarization subcycle, we are able to compute a measured asymmetry parameter for the superallowed transition as well. This quantity has been carefully measured previously [21] in a very similar experiment. For a number of reasons we expect systematic error in the present measurement to be worse than that in the previous. The present experiment uses a larger holding cell with much thicker walls. This allows us to achieve the high decay rates necessary to measure the very weak first-forbidden branch. The relatively thick walls of our cell cause significant scattering and energy loss of the β's. In order to accommodate the gamma detector, the solenoid magnet used in the previous measurement was modified resulting in a weaker and less uniform magnetic field. This, along with the larger cell radius, means that β's are not as well confined near the axis of the solenoid where the detectors are. This results in greater distortions in the β-spectrum shape and in the measured asymmetry.

These experimental distortions to the measured asymmetry can be accurately corrected by an energy-dependent factor which is *independent* of the size of the asymmetry. Since the end-point energies for the superallowed and first-forbidden transitions differ by only 5%, the correction factor for the two transitions is very similar. We therefore accept the previous measurement of the asymmetry parameter of the superallowed transition as accurate and use our measurement of that transition as a gauge of the systematic error in our measurement of the first-forbidden decay. This systematic error accounts for an 11% relative correction to the average asymmetry of the first-forbidden decay—a quantity with a relative statistical uncertainty of 74%.

D. Branching ratio

Since all β decays in the holding cell are recorded, the branching ratio for the first-forbidden transition may be

determined once the efficiency of the gamma detector over the cell volume is known. We surveyed the efficiency at 30 points within the volume of the holding cell using a mixed radionuclide point source [22]. At each point the efficiency at 110 keV was determined from a cubic spline interpolation of the efficiency for the four nearest γ-ray energies. The efficiency at 110 keV was then interpolated and averaged over the volume of the cell. Final uncertainty in the detector efficiency is 1.6% and is dominated by 1.1% uncertainty in the calibration source intensity.

Because the branching ratio is calculated from a ratio of counts in the "coincidence" ADC's to counts in the "singles" ADC's, there is a 5% correction for different dead times in the two systems. The dead-time correction is based on the average count rate during each acquisition subcycle. Another small adjustment is made for the fact that, since the end point of the first-forbidden branch is lower (by 110 keV) than the end point of the superallowed transition, a greater fraction of the first-forbidden decays fall below the software β-energy threshold. This correction was calculated from the fitted β-detector response function and is approximately 2%.

The 110 keV level is also populated by a γ transition following a β decay to the $3/2^+$ state at 1555 keV. The branching ratio for this transition is $(2.22 \pm 0.21) \times 10^{-5}$ and the subsequent branch to the 110 keV state is 5.1% [23,24]. Because of the low β-decay end point of 661 keV only 20% of β's from this branch will be above the software β-energy threshold. The contribution from this cascade to the measured branching ratio is then $(2.2 \times 10^{-5})\,(0.051)\,(0.2) \approx 0.002 \times 10^{-4}$.

During the asymmetry run the average trigger rate in the γ detector was 130 Hz; pulse width was 20 μs. This implies a loss in efficiency due to a pileup of $\sim$ 0.3%. Similarly pileup loss during calibration was $\sim$ 0.9%. A relative correction of $\sim$ 0.6% might therefore be applied toward decreasing the measured branching ratio. We neglect this small correction. Our measured branching ratio is then

$$\Gamma = (1.13 \pm 0.09) \times 10^{-4}.$$

This agrees well with a previous measurement by Adelberger *et al.* [12,13] of $\Gamma = (1.2 \pm 0.2) \times 10^{-4}$ and with another unpublished measurement performed at Princeton [25] of $\Gamma = (1.13 \pm 0.17) \times 10^{-4}$.

III. DISCUSSION

For the analysis of our measurement in terms of nuclear matrix elements we adopt the formalism of Behrens and Bühring [18] in which a multipole expansion is made of the nuclear current. The coefficients of this expansion are denoted ${}^A F_{KLS}(q^2)$ and ${}^V F_{KLS}(q^2)$ where q is the momentum transfer, K is the tensor rank, L the multipolarity, and $S = 0, 1$ is the spin of the spherical tensor operator; $S = 0$ terms arise from the time component of the current, $S = 1$ from the space components. V and A refer to *vector* and *axial-vector* currents. For first-forbidden transitions only the zeroth-order coefficients of an expansion in powers of (qR) are retained, $F_{KLS}(q^2) \approx F^{(0)}_{KLS}$. These so-called form-factor coefficients, ${}^A F^{(0)}_{KLS}$ and ${}^V F^{(0)}_{KLS}$ are the only quantities which can be determined from a β-decay experiment. The form-factor coefficients relevant to first-forbidden nonunique β decay are given in Table I along with their equivalent in Schopper Cartesian notation and in another common notation. The rank-2 form-factor ${}^A F^{(0)}_{211}$ is not allowed in the case $J_i = J_f = 1/2$.

The expansion of the electron radial wave function in powers of (αZ), $(m_e R)$, and (WR) introduces additional form-factor coefficients, $F^{(0)}_{KLS}(k, m, n, \rho)$, in which an additional radial dependence arising from the lepton wave function is included in the integral over the nuclear space coordinates. For our purposes these can be taken to be equal to a constant factor times the corresponding form factor without the additional radial dependence. For example, ${}^A F^{(0)}_{011}(1,1,1,1) = \mathcal{P}\,{}^A F^{(0)}_{011}$, where we take the ratio $\mathcal{P} = 1.095$ in all cases following calculations by Millener and Warburton [26,27]. Experimental observables are best expressed in terms of the following combinations of form-factor coefficients ([18], pp. 541-542):

$$A_0 = {}^A F^{(0)}_{000} \mp \frac{1}{3}\alpha Z\, {}^A F^{(0)}_{011}(1,1,1,1) - \frac{1}{3} W_0 R\, {}^A F^{(0)}_{011}\,, \tag{13}$$

$$B_0 = -\frac{1}{3}\, {}^A F^{(0)}_{011}\,, \tag{14}$$

$$\begin{aligned} C_0 = {} & -{}^V F^{(0)}_{101} \\ & \mp \frac{1}{3}\alpha Z \sqrt{\frac{1}{3}}\, {}^V F^{(0)}_{110}(1,1,1,1) - \frac{1}{3} W_0 R \sqrt{\frac{1}{3}}\, {}^V F^{(0)}_{110} \\ & \mp \frac{1}{3}\alpha Z \sqrt{\frac{2}{3}}\, {}^A F^{(0)}_{111}(1,1,1,1) + \frac{1}{3} W_0 R \sqrt{\frac{2}{3}}\, {}^A F^{(0)}_{111}\,, \end{aligned} \tag{15}$$

$$C_1 = -\frac{2}{3}\sqrt{\frac{2}{3}}\, {}^A F^{(0)}_{111}\,, \tag{16}$$

$$D_0 = -\frac{1}{3}\left[\sqrt{\frac{1}{3}}\, {}^V F^{(0)}_{110} + \sqrt{\frac{2}{3}}\, {}^A F^{(0)}_{111}\right], \tag{17}$$

$$E_0 = \sqrt{\frac{2}{3}}\, {}^V F^{(0)}_{110} + \sqrt{\frac{1}{3}}\, {}^A F^{(0)}_{111}\,, \tag{18}$$

TABLE I. Form-factor coefficients for first-forbidden nonunique β-decay (from Refs. [28,38]).

Form factor coefficient	Schopper Cartesian notation [a]	$\xi' y$, $\xi' v$, u, w, x, ...
${}^A F^{(0)}_{000}$	$\pm\lambda\langle\gamma_5\rangle$	$\xi' v$
${}^A F^{(0)}_{011}$	$\pm\lambda\langle i\boldsymbol{\sigma}\cdot\hat{\mathbf{r}}\rangle$	$-w/R$
${}^A F^{(0)}_{111}$	$\mp\lambda\sqrt{\frac{3}{2}}\langle\boldsymbol{\sigma}\times\hat{\mathbf{r}}\rangle$	$-\sqrt{\frac{3}{2}}u/R$
${}^V F^{(0)}_{101}$	$-\langle\boldsymbol{\alpha}\rangle$	$\xi' y$
${}^V F^{(0)}_{110}$	$\sqrt{3}\langle i\hat{\mathbf{r}}\rangle$	$-\sqrt{3}x/R$

[a] For $\beta^\mp$ decay.

$$F_0 = \sqrt{\frac{2}{3}}\,{}^V F_{110}^{(0)} - \sqrt{\frac{1}{3}}\,{}^A F_{111}^{(0)} , \tag{19}$$

where W_0 is the end-point total energy in units of $m_e c^2$. The shape factor is then given by ([18], p. 548)

$$C(W_e) = k_n(1 + aW_e + b/W_e + cW_e^2) , \tag{20a}$$

where for a first-forbidden transition with $J_i = J_f = 1/2$

$$k_n = A_0^2 + C_0^2 - 2\mu_1\gamma_1 R^2 C_1 D_0 + \frac{1}{9}(W_0 R)^2 E_0^2 + R^2\left[B_0^2 + D_0^2 - \frac{\lambda_2}{9}F_0^2\right] , \tag{20b}$$

$$k_n a = R\left[2C_0C_1 - \frac{2}{9}(W_0R)E_0^2\right] , \tag{20c}$$

$$k_n b = -2\mu_1\gamma_1 R(A_0B_0 + C_0D_0) , \tag{20d}$$

$$k_n c = R^2\left[C_1^2 + \frac{1}{9}(E_0^2 + \lambda_2 F_0^2)\right] , \tag{20e}$$

and

$$\gamma_1 = \sqrt{\{1 - (\alpha Z)^2\}}. \tag{20f}$$

The β-asymmetry parameter is given by ([18], pp. 548-549)

$$A = \pm[a_1^{(0)} + a_1^{(1)}(W_eR) + a_1^{(2)}(W_eR)^2] \tag{21a}$$

with

$$a_1^{(n)} = \left[\sqrt{\frac{1}{3}}b_{01}^{(1)}(n) - \frac{\sqrt{2}}{3}b_{11}^{(1)}(n)\right] , \tag{21b}$$

where

$$b_{01}^{(1)}(0) = 2\Lambda_1(A_0C_0 - R^2B_0D_0) + \hat{\eta}_{12}\frac{2\sqrt{2}}{3}R^2B_0F_0 , \tag{21c}$$

$$b_{01}^{(1)}(1) = 2\Lambda_1 A_0 C_1 - \frac{2}{3}\sqrt{2}\eta_{12}A_0F_0 , \tag{21d}$$

$$b_{01}^{(1)}(2) = 0 , \tag{21e}$$

$$b_{11}^{(1)}(0) = \sqrt{2}\Lambda_1(C_0^2 - R^2D_0^2) - \frac{2}{3}\hat{\eta}_{12}R^2D_0F_0 - \frac{\sqrt{2}}{18}R^2\Lambda_1 W_0^2 E_0^2 , \tag{21f}$$

$$b_{11}^{(1)}(1) = 2\sqrt{2}\Lambda_1 C_0 C_1 + \frac{2}{3}\eta_{12}C_0F_0 + \frac{\sqrt{2}}{9}(W_0R)\Lambda_1 E_0^2 , \tag{21g}$$

$$b_{11}^{(1)}(2) = \sqrt{2}\Lambda_1 C_1^2 + \frac{2}{3}\eta_{12}C_1F_0 - \frac{\sqrt{2}}{18}(\Lambda_1 E_0^2 - \lambda_2\Lambda_2 F_0^2) . \tag{21h}$$

The special Coulomb functions—μ_1, λ_2, Λ_1, Λ_2, η_{12}, $\hat{\eta}_{12}$—all close to unity, are taken from a tabulation by Behrens and Jänecke [28]. For R, the radius of a uniformly charged sphere with the equivalent rms charge radius of the nucleus, we adopt the value $R = 9.453 \times 10^{-3}\ \hbar/m_e c$ based on the expression given by Wilkinson ([29], p. 923). The end-point kinetic energy of the transition to the ground state is 2216.4 keV and the excitation energy of the $1/2^-$ level is 109.894 keV [30]. This gives end-point total energies of $W_0 = 5.1223$ for the first-forbidden transition, and $W_0 = 5.3374$ for the ground-state transition in units of $m_e c^2$.

The vector current form-factor coefficients, ${}^V F_{110}^{(0)}$ and ${}^V F_{101}^{(0)}$, can be determined from known rates of analogue gamma transitions in the parent and daughter nuclei using conserved vector current (CVC) theory and assuming good isospin symmetry. This leads to the following equations [26,31,32] for the case $T_i = T_f = 1/2$:

$${}^V F_{110}^{(0)} = -\frac{\sqrt{4\pi}}{R}\left\{[B(E1)]_f^{1/2} + [B(E1)]_i^{1/2}\right\} , \tag{22}$$

$${}^V F_{101}^{(0)} = -\sqrt{\frac{4\pi}{3}}\left\{q_f\,[B(E1)]_f^{1/2} + q_i\,[B(E1)]_i^{1/2}\right\} , \tag{23}$$

where i, f indicate values from the parent and daughter nucleus, and q is the gamma transition energy. The relevant transitions are shown in Fig. 5; energies and lifetimes are given in Table II. $B(E1)$ is defined by

$$B(E1) = \left(\frac{9}{16\pi\alpha}\right)\left(\frac{m_e c^2}{q}\right)^3\left(\frac{\hbar c}{m_e c^2}\right)\left(\frac{1}{c\tau_\gamma}\right) \tag{24}$$

and is dimensionless. We then have for the vector form-factor coefficients

$$\begin{aligned} {}^V F_{110}^{(0)} &= -0.044\,25 , \\ {}^V F_{101}^{(0)} &= -0.000\,089\,78 . \end{aligned}$$

The relative contribution of the vector form-factor coefficients to the total rate and asymmetry is negligible.

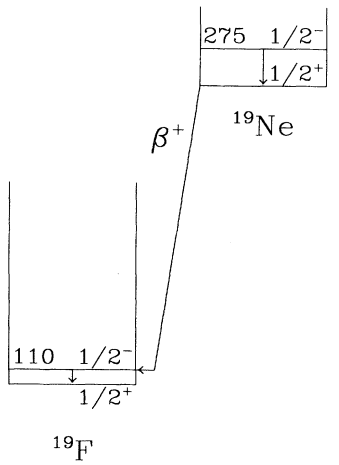

FIG. 5. Analogue gamma decays used to determine the vector form-factor coefficients for the first-forbidden β decay to the $1/2^-$ level in ^{19}F.

TABLE II. Analogue gamma transitions for the first-forbidden β decay of ^{19}Ne (from Ref. [39]).

Quantity	^{19}F	^{19}Ne	Units
q	109.894	275.09	keV
τ	853 ± 10	61.4 ± 3	ps
B(E1)	$(3.70 \pm 0.03) \times 10^{-9}$	$(3.27 \pm 0.15) \times 10^{-9}$	$\hbar = m_e = c = 1$
Γ/Γ_W	$(1.20 \pm 0.01) \times 10^{-3}$	$(1.07 \pm 0.05) \times 10^{-3}$	W.u.

With the final best-fit matrix elements their contribution to the total rank-1 term C_0 is about 2.5% [see Eq. (15)].

We now apply our experimental results to constrain the remaining three matrix elements. In this analysis we calculate χ^2 for the experimental asymmetry and shape factor data over a region of the space of matrix elements ${}^A F_{000}^{(0)}$ and ${}^A F_{111}^{(0)}$. The data for the shape factor are the β spectrum for the first-forbidden transition. This is compared to a theoretical spectrum convolved with the fitted detector response function as follows:

$$I_{\rm ff}(W) = \frac{\epsilon_\gamma}{C_{\rm g.s.}} A \int_1^{W_0} R(W,W')\, C_{\rm ff}(W') \times F(W',Z)\, g(W')\, {\rm d}W' , \qquad (25)$$

where $g(W) = (W_0 - W)^2 W (W^2-1)^{1/2}$, and $F(W,Z)$ is the Fermi function taken from a tabulation by Behrens and Jänecke [28]. $R(W,W')$ represents the response function derived from the fit to the ground-state spectrum; A is the amplitude factor from the fit to the spectrum of the superallowed branch; ϵ_γ is the calibrated efficiency of the HPGe γ detector for 110 keV γ rays originating in the holding cell. $C_{\rm g.s.}$ is the shape factor of the ground-state decay. We evaluate $C_{\rm g.s.}$ from the half-life of ^{19}Ne and the integrated phase space. We have

$$C_{\rm g.s.} = \left(\frac{2\pi^3 \ln 2}{G_\beta'^2}\right)\left(\frac{1}{t_{1/2}}\right)\left(\frac{1}{f_Z(W_0)}\right) . \qquad (26)$$

We use the values $f_Z(W_0) = 99.59$ from a parametrization for allowed decays by Wilkinson and Macefield [33], and $\frac{2\pi^3 \ln 2}{G_\beta'^2} = 6173$ s ([18], p. 446). With $t_{1/2} = 17.22 \pm 0.02$ s for the half-life of ^{19}Ne [30,34], we have $C_{\rm g.s.} = 3.600 \pm 0.003$. Figure 6 shows the measured β spectrum for the first-forbidden transition along with that calculated for the best-fit matrix elements. Figure 7 shows the measured and calculated β asymmetry.

The fit makes a model-independent determination of the single undetermined rank-1 form-factor coefficient ${}^A F_{111}^{(0)}$. However, because the dominant rank-0 term A_0 is a combination of the two rank-0 form-factor coefficients ${}^A F_{000}^{(0)}$ and ${}^A F_{011}^{(0)}$, it is not possible to constrain the timelike axial-vector term ${}^A F_{000}^{(0)}$ if ${}^A F_{011}^{(0)}$ is allowed to vary. It is possible, in principle, to isolate the contribution of ${}^A F_{011}^{(0)}$ using the energy dependence of the shape factor. The coefficient $k_n b$ [Eq. (20d)] is dominated by the term $A_0 B_0$; the total rank-0 term A_0 is nearly fixed by the branching ratio. By fitting to model data, we estimate that we would require 10 000 counts in a background-free β spectrum of the first-forbidden transition in order to determine ${}^A F_{011}^{(0)}$ and ${}^A F_{000}^{(0)}$ to within 10% of the total rank-0 matrix element. With our present signal-to-noise we would require 50 000 counts. Of course there is no need to have polarized ^{19}Ne for the shape-factor measurement.

In order to fit for the timelike axial-vector form-factor coefficient, we adopt the value ${}^A F_{011}^{(0)} = -0.186$ from a recent shell-model calculation by Warburton *et al.* [35]. Because ${}^A F_{011}^{(0)}$ occurs in combination with a small kine-

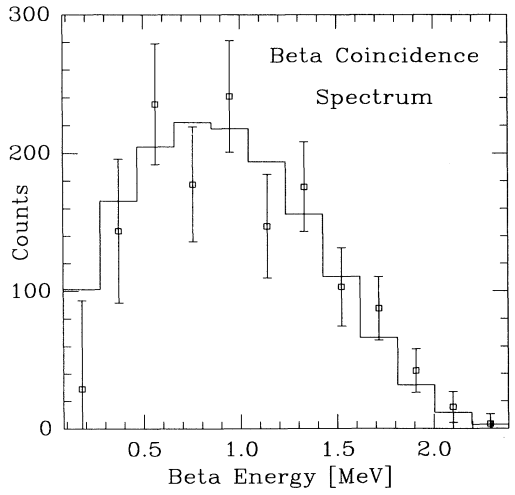

FIG. 6. Beta spectrum for the first-forbidden transition. The histogram is the convolved theoretical spectrum with the lowest χ^2 when ${}^A F_{011}^{(0)}$ is fixed.

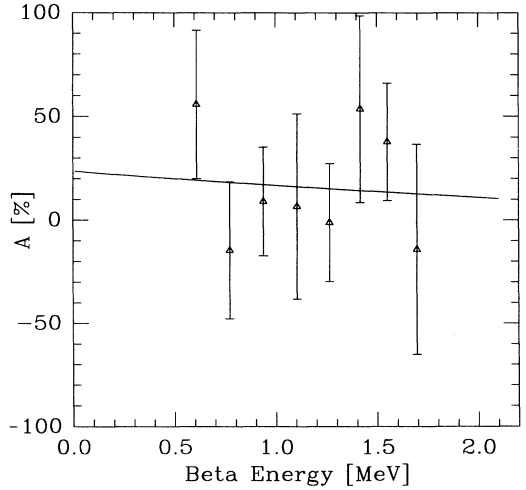

FIG. 7. Beta asymmetry of the first-forbidden transition. The line is the calculated asymmetry with the lowest χ^2 when ${}^A F_{011}^{(0)}$ is fixed.

matic factor its contribution to the dominant rank-0 term A_0 is only 6% of the total. The best-fit values and 1σ limits from the fit are

$$^{A}F^{(0)}_{000} = 0.0238 \pm 0.0009 ,$$
$$^{A}F^{(0)}_{111} = -0.14\ ^{+0.10}_{-0.08} .$$

It is usual to quote first-forbidden β-decay rates in terms of the integrated Fermi function f which satisfies the equation

$$ft = 6173 \text{ s} , \tag{27}$$

where t is the partial half-life of the transition and

$$f = \int_1^{W_0} C_R(W_e)\, F(Z, W_e)\, g(W_e)\, dW_e , \tag{28}$$

where $C_R(W_e)$ is the shape factor including the order-α radiative correction [36]. Matrix elements of different rank do not interfere in the shape factor; the total f may therefore be separated according to rank:

$$f = f^{(0)} + f^{(1)} . \tag{29}$$

Our 1σ limits correspond to

$$f = 0.0404\ ^{+.0032}_{-0.0031} ,$$
$$f^{(0)} = 0.0397\ ^{+0.0032}_{-0.0031} ,$$
$$f^{(1)} = 0.0007\ ^{+0.0009}_{-0.0007} ,$$

the total rank-1 contribution to the rate being $2 \pm 2\,\%$ (1σ limits).

Finally we calculate the isovector pion-exchange matrix element of V^{PNC}. From Eqs. (1) and (2) we obtain

$$\frac{\langle V^{\text{PNC}}_\pi \rangle}{f_\pi} = \left(\frac{\lambda M}{g_{\pi NN}}\right) \frac{\langle 1/2, 1/2 | 1, 0; 1/2, 1/2 \rangle}{\langle 1/2, 1/2 | 1, 1; 1/2, -1/2 \rangle} \times \left(\frac{\alpha}{\alpha + 1}\right) {}^{A}F^{(0)}_{000} . \tag{30}$$

If we adopt Haxton's value [37]

$$\alpha = \frac{^{A}F^{(0)}_{000}(\text{two-body})}{^{A}F^{(0)}_{000}(\text{one-body})} = 0.53 \pm 0.05$$

for the ratio of two- to one-body contributions to the timelike axial-vector matrix element, we obtain

$$\frac{\langle V^{\text{PNC}}_\pi \rangle}{f_\pi} = 0.51 \text{ MeV}.$$

This compares with Adelberger and Haxton's value of

$$\frac{\langle V^{\text{PNC}}_\pi \rangle}{f_\pi} = 0.49 \text{ MeV}.$$

The difference is partly due to differing estimates of the contribution of the matrix element $^{A}F^{(0)}_{011}$. In Haxton's calculation $^{A}F^{(0)}_{011}$ contributes about 3.5% of the total rank-0 matrix element and adds *constructively*. In our case, the contribution of $^{A}F^{(0)}_{011}$ is equal to about 6% of the total rank-0 matrix element and adds *destructively*. The difference in sign arises from the fact that the multipole expansion used by Haxton does not take account of the Coulomb field of the nucleus, except through the Fermi function $F(Z, W)$. $1/\sqrt{3}\ ^{A}F^{(0)}_{011}$ then occurs with a coefficient of

$$-\frac{W_0 R}{3} = -0.016 ,$$

whereas in Behrens and Bühring's treatment the corresponding coefficient is

$$\left(\frac{\alpha Z}{3}\mathcal{P} - \frac{W_0 R}{3}\right) = 0.024 - 0.016 = +0.008 .$$

IV. SUMMARY

The original calibration [4] of the isovector pion-exchange matrix element of V^{PNC} is confirmed and has been improved in several ways.

We have obtained an improved measurement of the branching ratio of $\Gamma = (1.13 \pm 0.09) \times 10^{-4}$ for the first-forbidden β^+ decay of ^{19}Ne to the $1/2^-$ state at 110 keV in ^{19}F. This is in good agreement with previous measurements and the uncertainty has been reduced by a factor of 2.

The measured β asymmetry of $\langle A \rangle = 17 \pm 12\,\%$ limits the contribution of rank-1 matrix elements to the branching ratio to be $2 \pm 2\,\%$. This is in agreement with the calculations in the original analysis, but this contribution had been estimated to be as much as $\sim 20\%$ in other nuclear structure calculations.

The measurement of the β asymmetry in combination with the branching ratio determines the total rank-0 and rank-1 matrix elements. Because two of the three rank-1 terms are known from CVC and the rates of analogue gamma transitions, this measurement effectively determines the third. A nuclear structure calculation is still required to separate the contribution of the two rank-0 terms in order to determine the timelike axial-vector matrix element. The additional constraint provided by the measurement of the β asymmetry should improve this calculation. Another benefit of an improved nuclear structure calculation will be a better determination of the ratio of two- to one-body contributions to the timelike axial-vector matrix element, α in Eq. (30) (also referred to as $\epsilon_{\text{mec}} - 1$ in some literature [38]). For this work we have used the value from the original analysis.

Finally, we point out that the parity mixing in ^{19}F is the result of isoscalar as well as isovector contributions. This calibration therefore does not place a definite limit on f_π, as it does in the case of ^{18}F. Since the ^{18}F results indicate a value of f_π which is almost an order of

magnitude smaller than the calculated "best value" of Desplanques *et al.* [1], it is important that another independent measurement be obtained. The ^{19}F result is the only other case of a "calibrated" measurement. It is an important component to be combined with other parity-violation measurements in order to determine the couplings of the PNC-NN interaction.

ACKNOWLEDGMENTS

The authors would like to thank E. K. Warburton and D. J. Millener for useful discussions about their shell-model calculations and for allowing us to use their unpublished results. This work was supported by the National Science Foundation.

[1] B. Desplanques, J. F. Donoghue, and B. R. Holstein, Ann. Phys. (N.Y.) **124**, 449 (1980).
[2] H. C. Evans *et al.*, Phys. Rev. Lett. **55**, 791 (1985).
[3] M. Bini, T. F. Fazzini, G. Poggi, and N. Taccetti, Phys. Rev. Lett. **55**, 795 (1985).
[4] E. G. Adelberger *et al.*, Phys. Rev. C **27**, 2833 (1983).
[5] K. Elsener *et al.*, Phys. Rev. Lett. **52**, 1476 (1984).
[6] E. D. Earle *et al.*, Nucl. Phys. **A396**, 221c (1983).
[7] C. L. Bennett, K. Krien, and M. M. Lowry, Bull. Am. Phys. Soc. **25**, 723 (1980).
[8] K. Kubodera, J. Delorme, and M. Rho, Phys. Rev. Lett. **40**, 755 (1978).
[9] J. Delorme, Nucl. Phys. **A374**, 541c (1982).
[10] W. C. Haxton, Phys. Rev. Lett. **46**, 698 (1981).
[11] D. H. Wilkinson, Nucl. Phys. **A377**, 474 (1982).
[12] E. G. Adelberger, C. D. Hoyle, H. E. Swanson, and R. D. von Lintig, Phys. Rev. Lett. **46**, 695 (1981).
[13] E. G. Adelberger *et al.*, Phys. Rev. C **24**, 313 (1981).
[14] E. J. Konopinski, *The Theory of Beta Radioactivity* (Clarendon Press, Oxford, 1966).
[15] D. J. Millener and E. K. Warburton, in *International Symposium on Nuclear Shell Models*, edited by M. Vallieres and B. A. Wildenthal (World Scientific, Singapore, 1985), p. 365.
[16] R. M. Baltrusaitis and F. P. Calaprice, Phys. Rev. Lett. **38**, 464 (1977).
[17] E. R. J. Saettler, Ph.D. thesis, Princeton University, 1992.
[18] H. Behrens and W. Bühring, *Electron Radial Wave Functions and Nuclear Beta Decay* (Clarendon Press, Oxford, 1982).
[19] W. Nelson *et al.*, SLAC Report 265, 1985, p. 1.
[20] D. W. O. Rogers, Nucl. Instrum. Methods A **227**, 535 (1984).
[21] D. F. Schreiber, Ph.D. thesis, Princeton University, 1982.
[22] National Bureau of Standards standard reference material 4275.
[23] E. G. Adelberger, in *Polarization Phenomena in Nuclear Physics - 1980*, (Fifth International Symposium, Santa Fe), Proceedings of the Fifth International Symposium on Polarization Phenomena in Nuclear Physics, AIP Conf. Proc. No. 69, edited by G. G. Ohlsen *et al.* (AIP, New York, 1981), pp. 1367–1383.
[24] *Table of Isotopes*, edited by E. Browne, J. M. Dairiki, R. E. Doebler, Virginia S. Shirley, and C. Micheal Lederer, (Wiley, New York, 1978).
[25] M. M. Lowry, R. T. Kouzes, F. P. Calaprice, and C. L. Bennett, Bull. Am. Phys. Soc. **25**, 492 (1981), results from M. M. Lowry, private communication.
[26] D. J. Millener, private communication.
[27] $\mathcal{P}_{\text{Behrens \& Bühring}} = \frac{3}{2}\mathcal{P}_{\text{Millener \& Warburton}}$.
[28] H. Behrens and J. Jänecke, *Numerical Tables for Beta-Decay and Electron Capture*, Landolt-Börnstein, New Series, Group I, Vol. 4 (Springer-Verlag, Berlin, 1969).
[29] D. H. Wilkinson, in *Nuclear Physics with Heavy Ions and Mesons,* 1977 Les Houches Lectures, edited by R. Bailin, M. Rho, and G. Ripka (North-Holland, Amsterdam, 1978), Vol. 2, pp. 877–1017.
[30] E. Browne, R. B. Firestone, and Virginia S. Shirley, *Table of Radioactive Isotopes* (Wiley, New York, 1986).
[31] These expressions are derived from Eqs. 10.70, 10.77, 9.74, and 9.77 in Behrens and Bühring [18], along with the relation $-{}^{\gamma}F_{101} = (qR/\sqrt{3})\,{}^{\gamma}F_{110}$ for the electromagnet current [32]. An overall sign for the form-factor coefficients is taken from shell-model calculations by Millener and Warburton [26].
[32] H. A. Smith and P. C. Simms, Phys. Rev. C **1**, 1809 (1970).
[33] D. H. Wilkinson and B. E. F. Macefield, Nucl. Phys. **A232**, 58 (1974).
[34] G. Azuelos and J. E. Kitching, Phys. Rev. C **12**, 563 (1975).
[35] E. K. Warburton, private communication. Because of the large cancellations involved, the uncertainty in the matrix element should be considered to be almost as large as the matrix element itself.
[36] See Behrens and Bühring ([18], pp. 431–432).
[37] E. G. Adelberger and W. C. Haxton, Annu. Rev. Nucl. Part. Sci. **35**, 501 (1985).
[38] E. K. Warburton, Phys. Rev. C **44**, 233 (1991).
[39] H. F. Schopper, *Weak Interactions and Nuclear Beta Decay* (North-Holland, Amsterdam, 1966).
[40] F. Ajzenberg-Selove, Nucl. Phys. **A300**, 1 (1978).